Observing Power-Law Dynamics of Position-Velocity Correlation in Anomalous Diffusion

Gadi Afek, Jonathan Coslovsky, Arnaud Courvoisier, Oz Livneh, and Nir Davidson
Department of Physics of Complex Systems, Weizmann Institute of Science, Rehovot 76100, Israel
(Received 30 April 2017; published 8 August 2017)

In this Letter, we present a measurement of the phase-space density distribution (PSDD) of ultracold ^{87}Rb atoms performing 1D anomalous diffusion. The PSDD is imaged using a direct tomographic method based on Raman velocity selection. It reveals that the position-velocity correlation function $C_{xv}(t)$ builds up on a time scale related to the initial conditions of the ensemble and then decays asymptotically as a power law. We show that the decay follows a simple scaling theory involving the power-law asymptotic dynamics of position and velocity. The generality of this scaling theory is confirmed using Monte Carlo simulations of two distinct models of anomalous diffusion.

DOI: 10.1103/PhysRevLett.119.060602

The phase-space density distribution (PSDD) contains information concerning the degrees of freedom of a system and allows calculation of any observable. An intriguing system to look at in this context is that of anomalous dynamics for which the mean square displacement scales as $\langle x^2\rangle \sim t^{2\alpha}$, with $\alpha \neq 1/2$. This type of dynamics, found in a wide variety of systems in nature ranging from dynamics of "bubbles" in denaturing DNA molecules [1], through fluctuations in the stock market [2], to models describing brief awakenings in the course of a night's sleep [3], is generally nonuniversal and system dependent [4–6].

A uniquely interesting model system for the study of anomalous diffusion is that of cold atoms diffusing in a dissipative 1D lattice, closely related to Lévy walks and motion in logarithmic potentials, displaying such phenomena as the breakdown of ergodicity and of equipartition, memory effects, and slow relaxation to equilibrium [6–23]. The major advantage of such a system is the high degree of control it enables over the physical parameters governing the dynamics. One of the fundamental insights that can be obtained from the PSDD of such a system is the phase-space cross correlation between position and velocity C_{xv}. C_{xv} can reveal the fingerprint of the underlying model and, in particular, is essential for understanding concepts and techniques such as adiabatic cooling in lattices [24], stochastic cooling [25], point source atom interferometry [26,27], and enhanced velocity resolution [28,29], alongside elementary notions in quantum mechanics [30]. These correlations have been surprisingly overlooked in both theory and experiment, perhaps due to the lack of a direct method for imaging the phase space of atomic clouds, which does not require cumbersome mathematical tools or a specific potential [31–35]. No analysis of the dynamics of the correlations has been reported to the best of our knowledge.

In this Letter, we analyze and measure the dynamics of the position-velocity correlation of an ensemble of classical particles, originating from a pointlike source and undergoing one-dimensional anomalous superdiffusion. The measurement is done using a new tomographic method for direct phase-space imaging, utilizing a combination of the straightforward tools of absorption imaging and the velocity sensitivity of Raman control. We obtain qualitative agreement with theory in the form of a scaling argument we derive, connecting the temporal asymptotics of the correlations with those of position and velocity. We verify the universality of the scaling law using two different types of Monte Carlo simulations.

The position-velocity correlation function is defined as

$$C_{xv}(t) \equiv \frac{\langle \delta\vec{x}(t)\cdot\delta\vec{v}(t)\rangle}{\sqrt{\langle \delta\vec{x}^2(t)\rangle\langle\delta\vec{v}^2(t)\rangle}}, \tag{1}$$

where for any observable $\mathcal{A}$ and PSDD $f(x,v)$, $\langle\mathcal{A}\rangle = \int \mathcal{A} f(x,v)dxdv$ and $\delta\mathcal{A} = \mathcal{A} - \langle\mathcal{A}\rangle$. Calculation for an initially uncorrelated ensemble of particles, reveals that $C_{xv}(t)$ asymptotically approaches unity for ballistic motion and decays as $1/\sqrt{t}$ for normal diffusion [36]. The inherent time scales depend strongly on the initial conditions of the ensemble, and their observation demands a pointlike atomic source.

For the general case of power-law dynamics and anomalous diffusion, we use Eq. (1) to derive a scaling argument, assuming power-law behavior of both $\langle\delta x^2(t)\rangle \sim t^{2\alpha}$ and $\langle\delta v^2(t)\rangle \sim t^{2\beta}$. The scaling of the numerator of Eq. (1) is calculated by taking the derivative

$$\langle\delta x\cdot\delta v\rangle \sim \frac{d\langle\delta x^2\rangle}{dt} \sim t^{2\alpha-1}. \tag{2}$$

The denominator of Eq. (1) gives $t^{\alpha+\beta}$. Together this yields

$$C_{xv}(t) \sim t^{\alpha-\beta-1} \sim t^{\gamma}. \tag{3}$$

The $(\alpha,\beta) = (1/2, 0)$ normal-diffusive limit and $(\alpha,\beta) = (1,0)$ ballistic limit give $\gamma = -1/2$ and $\gamma = 0$, respectively,

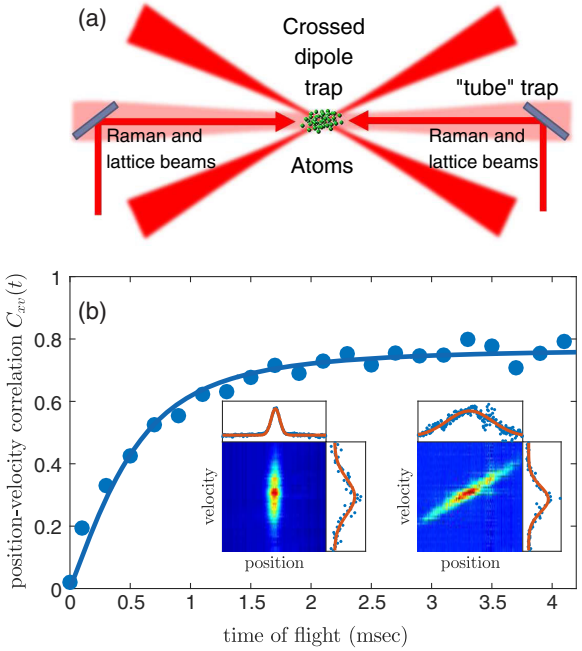

FIG. 1. (a) A sketch of the experimental setup. Laser-cooled ^{87}Rb atoms are loaded into a crossed optical dipole trap and evaporated. They are then transferred into a single-beam red-detuned tube trap and perform anomalous diffusion in a dissipative optical lattice at a certain lattice depth for a given time. Their phase-space distribution is then measured using the tomographic method described in the text. (b) Measured position-velocity correlation for ballistically expanding atoms. Solid line represents the fit to Eq. (4). Left (right) insets show short (long) time phase-space reconstruction. Integrals over the velocity and position axes are presented along with a fit to a Gaussian, taken for ballistic expansion after 0.1 (4.1) msec time of flight. The shearing of phase-space indicates correlations between position and velocity.

indicating a decay of $1/\sqrt{t}$ for normal diffusion and saturation at a nonzero value for ballistic motion.

In the experiment [Fig. 1(a)], a cloud of $\sim 10^5$ ^{87}Rb atoms is loaded into a crossed dipole trap from a Raman-sideband cooled magneto-optical trap. After a short evaporation and thermal equilibration stage, the pointlike atomic cloud (~ 30 μm in size, $T \approx 10$ μK) is loaded adiabatically into a single-beam, elongated dipole trap providing confinement in the radial axis (for details, see [16]). The atoms then undergo anomalous superdiffusion for lattice exposure time t, in a 1D Sisyphus lattice of depth U_0 [37], originating from a distributed feedback diode laser detuned -66 MHz relative to the transition between states $5^2S_{1/2}$, $F = 2$ and $5^2P_{3/2}$, $F' = 3$.

Then, we perform tomographic phase space imaging by transferring atoms whose velocity lies within a narrow velocity class, from the $|F = 1\rangle$ lower hyperfine ground state to the upper ground-state level $|F = 2\rangle$ using a Raman velocity-selective π pulse with two counter-propagating beams. The center of the selected velocity class is scanned by varying the two-photon detuning of the pulse, and the Rabi frequency sets its width [38]. These atoms are imaged onto a CCD camera using state-selective absorption imaging. The measured PSDD is depicted, for ballistic expansion (i.e., with $U_0 = 0$), in the left and right insets of Fig. 1(b) for short (0.1 msec) and long (4.1 msec) times, respectively, revealing the expected shearing of the PSDD. The position-velocity correlation is extracted from the data [39] and shown in Fig. 1(b) as a function of free propagation time t (termed "time of flight" for $U_0 = 0$). Correlations brought about by ballistic expansion, starting with an uncorrelated Gaussian phase-space are given by [30]

$$C_{x,v}(t) = \frac{\omega_{\mathrm{osc}} t}{\sqrt{1 + \omega_{\mathrm{osc}}^2 t^2}}, \tag{4}$$

where $\omega_{\mathrm{osc}} \equiv \sigma_v(t = 0)/\sigma_x(t = 0)$ sets, under thermal equilibrium, the ratio between the initial standard deviation of the velocity distribution, σ_v and that of the position distribution σ_x. It also represents the oscillation frequency in the trap prior to the release. This parameter sets the initial slope of the buildup of the correlations.

To establish the validity of the new tomographic method, we test it on this textbook case. We fit the ballistic expansion phase-space tomography data shown in Fig. 1(b) to Eq. (4), and obtain a value of $\omega_{\mathrm{osc}} = 2\pi \times (213 \pm 15)$ Hz, in excellent agreement with the value obtained independently of $\omega_{\mathrm{osc}} = 2\pi \times (230 \pm 3)$ Hz, measured by giving a small kick to the trapped atoms, and imaging the oscillations in the trap. The measured zero-time correlation value is consistent with zero up to the measurement error, as expected from an equilibrated cloud. The saturation value obtained from the fit, $C_\infty = 0.77 \pm 0.01$, is subunity due to a broadening effect arising from a finite two-photon Rabi frequency required to obtain good SNR. The broadening in the correlation is a function of the ratio between the spectral width of the velocity-selective Raman π pulse (rescaled by $2k_L$, the wave number of the Raman laser) and that of the velocity distribution. As the Rabi frequency becomes small compared to the width of the velocity distribution the measured correlation becomes closer to the real value. The Rabi frequency selected for the experiment reflects the tradeoff between minimizing the broadening and obtaining good SNR. Calibrating this effect, we rescale the data such that $C_\infty = 1$. Figure 2 presents the measured, rescaled position-velocity correlations as a function of lattice exposure time t and lattice depth in linear (a) and log-log (b) scales, ranging from ballistic to normal diffusion. It shows the initial buildup and sequential decay of the correlations.

To develop a theoretical description, we first consider the limits of normal diffusion and ballistic expansion, using the Langevin equation approach to normal Brownian motion [36,40,42]. The instantaneous acceleration of a particle in a medium is given by $\dot{\vec{v}} = -\Gamma\vec{v} + \vec{\mathcal{A}}$, where $\vec{v}$ is the velocity

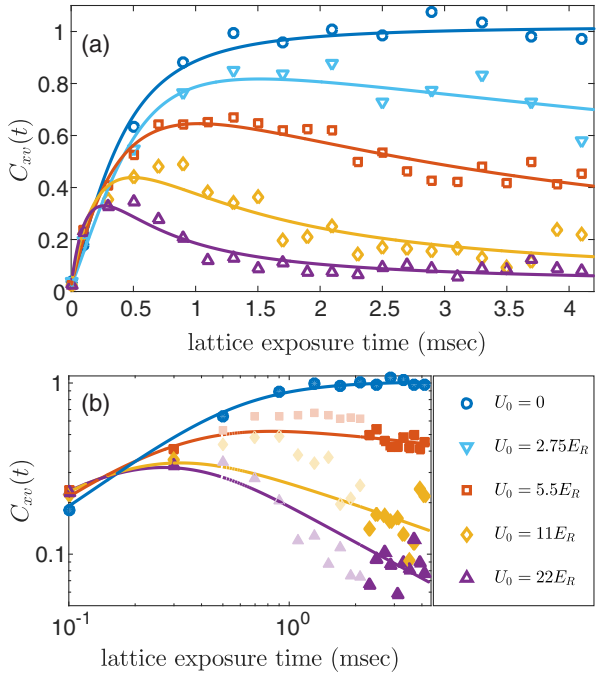

FIG. 2. (a) Rescaled position-velocity correlations as a function of lattice exposure time and lattice depth. Colors and symbols indicate different lattice depths, U_0. E_R is the recoil energy. At short times, the correlations build up and are later quenched at varying rates, depending on the anomalous dynamics. Solid lines indicate the fit to the interpolation formula of Eq. (9). (b) Fit to the interpolation formula of Eq. (9) on a log-log scale, excluding interim times $0.5 \le t \le 2.1$ msec. Shaded symbols are excluded points. The $U_0 = 0$ data set has no exclusions.

vector, Γ is the drag coefficient setting the time scale for transition between the ballistic and diffusive regimes, and $\vec{\mathcal{A}}$ is the Langevin random acceleration. For simplicity, we assume $\langle x \rangle = \langle v \rangle = 0$, hence, $\delta x = x$ and $\delta v = v$. The numerator of Eq. (1) can be calculated by noticing that

$$\frac{d}{dt}\langle \vec{x} \cdot \vec{v} \rangle = -\Gamma \langle \vec{x} \cdot \vec{v} \rangle + \langle \vec{v}^2 \rangle, \tag{5}$$

where, due to the randomness of the Langevin acceleration, $\langle \vec{x} \cdot \vec{\mathcal{A}} \rangle = 0$. $\langle \vec{v}^2 \rangle$ is given by

$$\langle \vec{v}^2 \rangle = \sigma_{v_0}^2 + (\sigma_{v_{\rm eq}}^2 - \sigma_{v_0}^2)(1 - e^{-2\Gamma t}), \tag{6}$$

with $\sigma_{v_0}^2$ denoting the initial variance of the velocity distribution, and $\sigma_{v_{\rm eq}}^2 = \sigma_v^2(t \to \infty)$. Substituting into Eq. (5) and solving under an uncorrelated initial condition yields

$$\langle \vec{x}(t) \cdot \vec{v}(t) \rangle = \frac{e^{-2\Gamma t}(e^{\Gamma t} - 1)[\sigma_{v_{\rm eq}}^2 (e^{\Gamma t} - 1) + \sigma_{v_0}^2]}{\Gamma}. \tag{7}$$

Calculating the terms in the denominator [36,40] under the initial conditions $\langle \vec{x}^2(0) \rangle = \sigma_{x_0}^2$ and $d\langle \vec{x}^2 \rangle / dt|_{t=0} = 0$, and setting $\sigma_{v_0}^2 = \sigma_{v_{\rm eq}}^2$ (see [39] for full expression), we obtain

$$C_{xv}(t) = \frac{e^{-\Gamma t/2}(e^{\Gamma t} - 1)}{\{2 + e^{\Gamma t}[(\Gamma/\omega_{\rm osc})^2 + 2\Gamma t - 2]\}^{1/2}}. \tag{8}$$

Equation (8) reveals the initial linear rise in correlation due to the ballistic time scale of the dynamics and the asymptotic decay $\sim t^{-1/2}$ of the normal-diffusive correlations. The ballistic regime [Eq. (4)] is obtained from it by taking the $\Gamma \to 0$ limit.

Equation (8) can be generalized to account for anomalous diffusion and, hence, the power-law decay anticipated by Eq. (3) as

$$C_{xv}(t) = \frac{e^{-\Gamma t/2}(e^{\Gamma t} - 1)}{\{2 + e^{-\Gamma t/2\gamma}[(\Gamma/\omega_{\rm osc})^{-1/\gamma} + 2\Gamma t - 2]\}^{-\gamma}}. \tag{9}$$

This preserves $C_{xv} \sim t^{\gamma}$ at long times and the initial $C_{xv} \sim t$ at short times. It recovers Eq. (8) for $\gamma = -1/2$. In Figs. 2(a) and 2(b), we show, in solid lines, the fit of this function to the data with γ, $\omega_{\rm osc}$ and Γ as fit parameters [39]. There exist two time scales and two temporal scalings. The buildup scales linearly in time and saturates at unity with a time scale of $1/\omega_{\rm osc}$. The decay scales like t^{γ} with a time scale of $1/\Gamma$. The transition between the buildup and decay occurs at a time scale τ_m, which is approximately the average $(1/\omega_{\rm osc} + 1/\Gamma)/2$ [39]. Henceforth, it is evident that observing the short time correlation dynamics requires τ_m to be within the measurement time.

Figure 3(a) presents the position variance $\langle \delta x^2(t) \rangle$, for various lattice depths. The position distribution is obtained by integrating over the velocity axis of the tomographic phase-space images [see insets of Fig. 1(b)]. Fitting $\langle \delta x^2(t) \rangle - \langle \delta x^2(0) \rangle \sim t^{2\alpha}$ reveals that the entire superdiffusive regime is accessible in the experiment, as seen in the inset, bearing qualitative agreement with [16]. Figure 3(b) presents the decay exponent γ extracted from the fits of Fig. 2 as a function of $\alpha - 1$. The velocity distribution equilibrates at a fast time scale ($1/\Gamma < 1$ msec) to a steady-state value, meaning $\beta \approx 0$ [43]. The results (empty symbols) follow the trend of the scaling argument prediction of Eq. (3) but are significantly beneath it. Excluding the intermediate times $0.5 \le t \le 2.1$ msec from the fit yields qualitatively similar results, but with better agreement to the scaling argument (full symbols). This indicates that our interpolation function [Eq. (9)] describes the short and long time dynamics well but fails to describe the intermediate times. To test the generality of our scaling argument, we numerically study the dynamics of the position-velocity correlations within the framework of two distinct models featuring anomalous diffusion. The first describes semiclassical atomic motion in a 1D Sisyphus lattice [19], using the Langevin phase-space equations

$$\dot{x} = v, \qquad \dot{v} = -\frac{v}{1 + v^2} + \sqrt{2\mathcal{D}}\xi(t). \tag{10}$$

The white noise term $\xi(t)$ is Gaussian and has zero mean. The initial conditions are Gaussian, uncorrelated

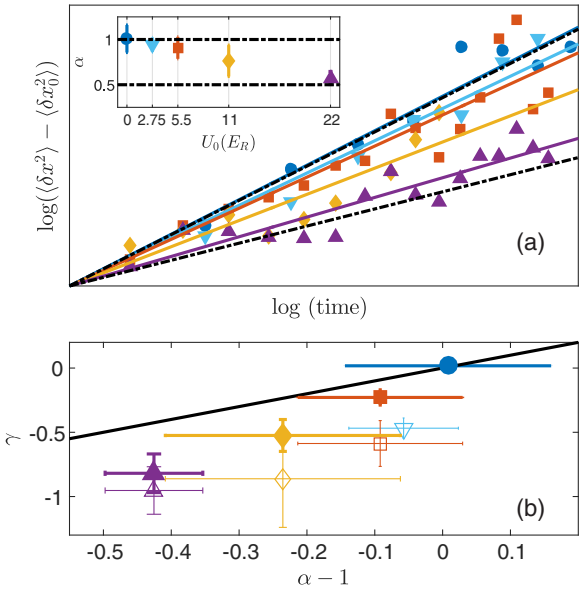

FIG. 3. (a) The variance of the position as a function of time on a log-log scale for various lattice depths, U_0. Solid lines are linear fits, whose slope is summarized in the inset, bearing good qualitative agreement with [16]. The data are shifted to cross at the origin. Black dotted lines represent the ballistic and normal-diffusive limits, showing that the entire superdiffusive regime is accessible. (b) Experimental demonstration of the scaling relation of Eq. (3) for the case of $\beta = 0$ (relaxed velocity dynamics). The exponent of the correlation, γ, extracted from fitting the interpolation function of Eq. (9) to the data of Fig. 2(a), is plotted in empty symbols as a function of $\alpha - 1$. The full symbols represent a fit excluding $0.5 \leq t \leq 2.1$ msec. The colors and shapes correspond to the lattice depths as in Fig. 2. The solid line is the theoretical scaling relation.

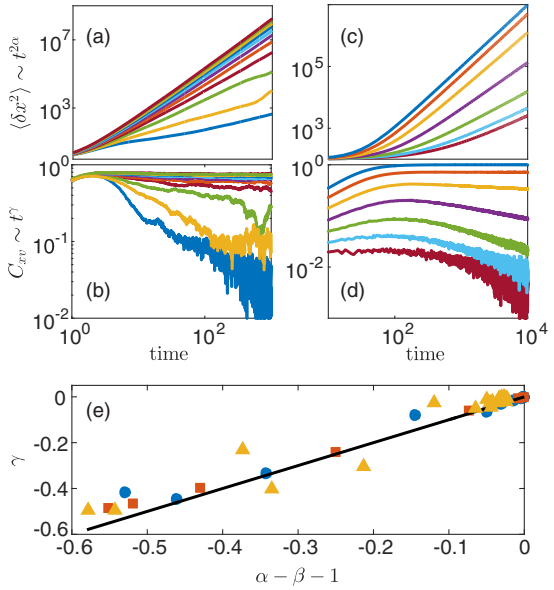

FIG. 4. Results of numerical Monte Carlo simulations of two anomalous diffusion models. (a) $\langle \delta x^2 \rangle$ as a function of time for different lattice depths, corresponding to the range of super-diffusive behavior. Larger slopes correspond to shallower lattices. A linear fit to the long-time data enables extraction of α. (b) Position-velocity correlations, showing the predicted power-law dependence. Stronger decay corresponds to deeper lattice. (a), (b) are obtained using the Langevin simulation of Eq. (10). (c), (d) Similar behavior, obtained from the Lévy walk simulation. Larger slopes correspond to smaller γ_0 in (c), stronger decay corresponds to larger γ_0 in (d). (e) Validation of the scaling relation $\gamma = \alpha - \beta - 1$. Light blue circles: preequilibrated dynamics in the Langevin simulation ($\beta = 0$), red squares: Lévy simulation (inherently preequilibrated, $\beta = 0$), and orange triangles: velocity dynamics in the Langevin simulation ($\beta \neq 0$).

distributions of unity standard deviation in both velocity and position. The diffusion constant is related to the depth of the lattice by $\mathcal{D} = cE_R/U_0$, where c is a dimensionless parameter of order 10 [7,8]. Figure 4(a) presents the simulated size of the cloud as a function of time and diffusion constant for $N = 10^4$ atomic trajectories. The power-law dependence $\langle x^2 \rangle \sim t^{2\alpha}$ is evident. The width of the velocity distribution scales like a power law in time [14]. The position-velocity correlation is calculated using the definition [Eq. (1)], and shown in Fig. 4(b). We fit the long-time decay of the correlation to t^{γ} and plot γ as a function of $\alpha - \beta - 1$ in Fig. 4(e), for two distinct scenarios, one where the velocities are initialized in some arbitrary initial size (orange triangles) and one where they are initialized at their steady-state value corresponding to each lattice depth, setting $\beta = 0$ (blue circles). The second simulation is a Lévy walk simulation [6], where particles are initialized in an uncorrelated Gaussian phase space and proceed to perform walks of durations τ, drawn from a unity-scaled Lomax distribution $\psi_{\gamma_0}(\tau) = \gamma_0/(1+\tau)^{1+\gamma_0}$. The width of the velocity distribution remains constant throughout the simulation ($\beta = 0$). $1 < \gamma_0 < 2$ gives access to the superdiffusive regime. Figure 4(c) shows the size of the cloud as a function of time and Fig. 4(d) the power-law decay of the correlations. Figure 4(e) shows the summary of the relation between the exponents α, β, and γ obtained using this method (red squares). All the simulation results for the two distinct anomalous diffusion models agree well with theory, indicating the generality of our scaling argument [Eq. (3)].

In summary, we present a measurement of the initial buildup and sequential decay of position-velocity correlations for a system of cold atoms performing anomalous superdiffusion. We find that the correlations decay asymptotically with a power-law exponent relating to the power-law exponents of the position variance and the velocity variance in qualitative agreement with a simple scaling argument we derive. The universality of the scaling law is validated using Monte Carlo simulations of two distinct models of anomalous diffusion. This universal relation between the long time decay of C_{xv} and other exponents that are easier to measure can be used to infer C_{xv} for systems where it cannot be measured directly. The position-velocity correlations are obtained using a new direct method to

measure the phase-space density distribution that can be used to access different types of phenomena such as deviations from the equipartition theorem [22,23] for the nonequilibrium steady-state scenario of the discussed system with the addition of an underlying harmonic potential, and to probe phase-space correlations in systems of a quantum nature, described by a single wave function [30,44]. The short-time dynamics in anomalous diffusion is model dependent and nontrivially experimentally accessible [45]. Our work invites theoretical analysis of the correlation function as a fingerprint of the details of the underlying model.

The authors would like to thank Eli Barkai, Andreas Dechant, and Erez Aghion for valuable theoretical input and Yoav Sagi, Hagai Edri, and Noam Matzliah for discussions.

[1] A. Bar, Y. Kafri, and D. Mukamel, Phys. Rev. Lett. **98**, 038103 (2007).
[2] V. Plerou, P. Gopikrishnan, L. A. Nunes Amaral, X. Gabaix, and H. E. Stanley, Phys. Rev. E **62**, R3023 (2000).
[3] C.-C. Lo, L. A. N. Amaral, S. Havlin, P. C. Ivanov, T. Penzel, J.-H. Peter, and H. E. Stanley, Europhys. Lett. **57**, 625 (2002).
[4] R. Metzler and J. Klafter, Phys. Rep. **339**, 1 (2000).
[5] I. M. Sokolov, Soft Matter **8**, 9043 (2012).
[6] V. Zaburdaev, S. Denisov, and J. Klafter, Rev. Mod. Phys. **87**, 483 (2015).
[7] Y. Castin, J. Dalibard, and C. Cohen-Tannoudji, in *Light Induced Kinetic Effects on Atoms, Ions and Molecules: Proceeding of the Workshop Held in Marciana Marina, Elba Island, Italy, May 2–5, 1990* (ETS Editrice, Pisa, 1991).
[8] S. Marksteiner, K. Ellinger, and P. Zoller, Phys. Rev. A **53**, 3409 (1996).
[9] H. Katori, S. Schlipf, and H. Walther, Phys. Rev. Lett. **79**, 2221 (1997).
[10] E. Lutz, Phys. Rev. A **67**, 051402 (2003).
[11] E. Lutz, Phys. Rev. Lett. **93**, 190602 (2004).
[12] J. Jersblad, H. Ellmann, K. Stöchkel, A. Kastberg, L. Sanchez-Palencia, and R. Kaiser, Phys. Rev. A **69**, 013410 (2004).
[13] P. Douglas, S. Bergamini, and F. Renzoni, Phys. Rev. Lett. **96**, 110601 (2006).
[14] D. A. Kessler and E. Barkai, Phys. Rev. Lett. **105**, 120602 (2010).
[15] O. Hirschberg, D. Mukamel, and G. M. Schütz, Phys. Rev. E **84**, 041111 (2011).
[16] Y. Sagi, M. Brook, I. Almog, and N. Davidson, Phys. Rev. Lett. **108**, 093002 (2012).
[17] D. A. Kessler and E. Barkai, Phys. Rev. Lett. **108**, 230602 (2012).
[18] A. Dechant and E. Lutz, Phys. Rev. Lett. **108**, 230601 (2012).
[19] E. Barkai, E. Aghion, and D. A. Kessler, Phys. Rev. X **4**, 021036 (2014).
[20] A. Dechant, E. Lutz, D. A. Kessler, and E. Barkai, Phys. Rev. X **4**, 011022 (2014).
[21] P. C. Holz, A. Dechant, and E. Lutz, Europhys. Lett. **109**, 23001 (2015).
[22] A. Dechant, D. A. Kessler, and E. Barkai, Phys. Rev. Lett. **115**, 173006 (2015).
[23] A. Dechant, S. T. Shafier, D. A. Kessler, and E. Barkai, Phys. Rev. E **94**, 022151 (2016).
[24] A. J. Kerman, V. Vuletić, C. Chin, and S. Chu, Phys. Rev. Lett. **84**, 439 (2000).
[25] M. G. Raizen, J. Koga, B. Sundaram, Y. Kishimoto, H. Takuma, and T. Tajima, Phys. Rev. A **58**, 4757 (1998).
[26] S. M. Dickerson, J. M. Hogan, A. Sugarbaker, D. M. S. Johnson, and M. A. Kasevich, Phys. Rev. Lett. **111**, 083001 (2013).
[27] G. W. Hoth, B. Pelle, S. Riedl, J. Kitching, and E. A. Donley, Appl. Phys. Lett. **109**, 071113 (2016).
[28] A. B. Henson, S. Gersten, Y. Shagam, J. Narevicius, and E. Narevicius, Science **338**, 234 (2012).
[29] F. Damon, F. Vermersch, J. G. Muga, and D. Guéry-Odelin, Phys. Rev. A **89**, 053626 (2014).
[30] R. W. Robinett, M. A. Doncheski, and L. C. Bassett, Found. Phys. Lett. **18**, 455 (2005).
[31] C. Kurtsiefer, T. Pfau, and J. Mlynek, Nature (London) **386**, 150 (1997).
[32] T. Pfau and C. Kurtsiefer, J. Mod. Opt. **44**, 2551 (1997).
[33] A. Del Campo, V. I. Manko, and G. Marmo, Phys. Rev. A **78**, 025602 (2008).
[34] S. K. Lee, M. S. Kim, C. Szewc, and H. Ulbricht, New J. Phys. **14**, 045001 (2012).
[35] S. Zhou, J. Chabé, R. Salem, T. David, D. Groswasser, M. Keil, Y. Japha, and R. Folman, Phys. Rev. A **90**, 033620 (2014).
[36] D. T. Gillespie and E. Seitaridou, *Simple Brownian Diffusion: An Introduction to the Standard Theoretical Models* (Oxford University Press, Oxford, 2012).
[37] It has been shown in [7] that the dipole potential depth of the lattice is the sole parameter governing the asymptotic dynamics.
[38] M. Kasevich, D. S. Weiss, E. Riis, K. Moler, S. Kasapi, and S. Chu, Phys. Rev. Lett. **66**, 2297 (1991).
[39] See Supplemental Material at http://link.aps.org/supplemental/10.1103/PhysRevLett.119.060602, which includes Refs. [36,40,41].
[40] R. Pathria, *Statistical Mechanics* (Butterworth Heinemann, Oxford, United Kingdom, 2006).
[41] K. Moler, D. S. Weiss, M. Kasevich, and S. Chu, Phys. Rev. A **45**, 342 (1992).
[42] J. Luczka, P. Talkner, and P. Hanggi, Physica (Amsterdam) **278A**, 18 (2000).
[43] Theory predicts $\beta > 0$ for shallow lattices; however, in our limited measurement time, we cannot observe this.
[44] T. Schweigler, V. Kasper, S. Erne, I. Mazets, B. Rauer, F. Cataldini, T. Langen, T. Gasenzer, J. Berges, and J. Schmiedmayer, Nature (London) **545**, 323 (2017).
[45] S. Kheifets, A. Simha, K. Melin, T. Li, and M. G. Raizen, Science **343**, 1493 (2014).